RSC Advances

PAPER

View Article Online
View Journal | View Issue

Cite this: *RSC Adv.*, 2014, **4**, 44229

Applications of mesoporous titanium phosphonate functionalized with carboxylic groups

Dongdong Li* and Yuping Zhang

Received 10th July 2014
Accepted 28th August 2014

DOI: 10.1039/c4ra06952h

www.rsc.org/advances

Mesoporous titanium phosphonate functionalized with –COOH was synthesized by a simple co-condensation process with the use of 2-phosphonoacetic acid and titanium tetrachloride under acid conditions. The obtained mesoporous materials show high surface area and large pore volume, which were supported by XRD, TEM, SEM and N_2 adsorption analysis. The integrity of the organophosphonate groups were further characterized by FTIR and NMR. Palladium nanoparticles were successfully supported onto the materials combined with a metal adsorption–reduction procedure, showing high activity for the Suzuki reaction. Furthermore, the obtained catalyst can be recovered and reused without significant decrease in catalytic activity.

Introduction

Inorganic–organic hybrid materials have been a hot research topic because of their combining properties of the inorganic and organic components.[1] These types of materials have the advantage of possessing a uniform distribution of functional organic groups within their framework, which allows us to tailor their density, chemical reactivity, and thermal stability.[2] To date, a large number of hybrid porous materials with various chemical compositions and organic groups have been well documented, showing interesting properties, such as catalysts and adsorbents.[3] Since the first periodic mesoporous organosilicas (PMOs) was reported in 1999, the preparation of nonsilica-based inorganic–organic hybrid mesoporous materials has been regarded as one of the recent breakthroughs.[4] Compared with the silica-based materials, metal organophosphonates are more promising because of their unique properties, such as proton conductivity, nonlinear optical effects, electron transfer, topochemical reactivity and photochromism.[5]

Carboxylic acid is a well-known reactive group, so carboxyl functionalized mesoporous materials are of significant interest for applications in separation, adsorption, catalysis, drug delivery, and nanotechnology because of the created negative charge and polarity.[6] Traditional carboxyl-modified mesoporous materials are more concentrated in silicon-based materials.[7] To date, carboxylic acid functionalized mesoporous phosphonate has been applied to enzyme adsorption, such as Shi *et al.* who have prepared mesoporous aluminum organophosphates with chiral L-proline groups in the pores.[8] Carboxylic groups have strong interaction with cationic species in aqueous solution, which could serve as anchor sites for adsorbing metal cations.[9]

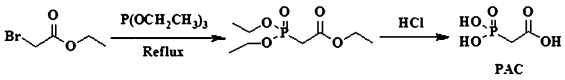

Scheme 1 The synthetic route of PAC.

In this work, we first prepared 2-phosphonoacetic acid (PAC) according to the synthetic route as shown in Scheme 1. Then, we synthesized high surface area mesoporous titanium phosphonate functional with –COOH by a simple co-condensation process. The synthesized material was fully characterized using XRD, TEM, N_2 adsorption, NMR and FTIR. This mesoporous titanium phosphonate material exhibited high adsorbing ability on Pd nanoparticles for catalysis, making it a promising reaction carrier for practical applications.

Experimental section

Materials

Titanium tetrachloride (Tianjin Fengchuan Chemical Co., Ltd.), ethyl bromoacetate (J&K Chemical Co., Ltd.), triethyl phosphite (Chengdu Kelong Chemical Reagent Factory), hexadecyltrimethylammonium Chloride (CTAC, Tianjin Guangfu Chemical Co., Ltd.). All the materials were purchased without further purification.

Synthesis of ethyl-2-(diethoxyphosphoryl)acetate

A mixture of ethyl bromoacetate (2.2 g, 13.2 mmol) and triethyl phosphite (2.19 g, 13.2 mmol) was heated in a flame-dried flask to 90 °C for 10 h. The mixture was allowed to cool down to afford the desired product (2.83 g, 98%). ^{1}H NMR ($CDCl_3$, 300 MHz): δ

Department of Materials Science, Jilin University, Changchun, 130012, P. R. China. E-mail: lidongdong@jlu.edu.cn; Tel: +86-43185168540

1.297–1.375 (m, 9H), 2.923–3.000 (d, 2H), 4.130–4.241 (m, 6H). ^{13}C NMR (75 MHz, $CDCl_3$): 165.7, 62.6, 61.4, 33.5, 16.2, 14.0.

Synthesis of 2-phosphonoacetic acid (PAC)

Ethyl-2-(diethoxyphosphoryl)acetate (2.3 g, 10 mmol) and HCl (50 mL) was heated to reflux for 9 h, after cooling to room temperature the water was removed by distillation under reduced pressure. The crude product was added to ethyl acetate (100 mL) to stir at room temperature, then the white suspension was filtrated and washed with ethyl acetate, the resulting white powder was dried under vacuum (1.3 g, 93%). ^{1}H NMR (D_2O, 300 MHz): δ 2.950–3.019 (d, 2H). ^{13}C NMR (75 MHz, D_2O): 168.7, 32.3.

Synthesis of mesoporous titanium phosphonate functionalized with carboxylic groups (TiP)

In a typical synthesis procedure, CTAC (0.2 g, 0.625 mmol) and PAC (0.14 g, 1 mmol) were added into deionized water (9 mL) with vigorous stirring, and then $TiCl_4$ (P/Ti molar ratio: 1.2/1) of ethanol (2 mL) solution was added very slowly. The mixture was placed in an ice water bath to slow down the hydrolysis of $TiCl_4$, and the pH value was adjusted to be *ca.* 4.0. A homogenous colloidal solution was obtained after another 3 h of stirring. The obtained mixture was transferred to a Teflon-lined autoclave and crystallized statically at 120 °C under autogenous pressure for about 24 h. Then, the obtained precipitate was filtered and refluxed in ethanol for 24 h to remove the template. The mesoporous titanium phosphonate functionalized with carboxylic groups was obtained after drying at 60 °C, marked as TiP.

Catalysis experiments

Preparing palladium nanoparticles on the support TiP:palladium(II) chloride (10 mg, 0.056 mmol) and NaCl (70 mg, 1.2 mmol) were dissolved in water (10 mL) for 15 min under a nitrogen atmosphere. TiP (200 mg) was then added to the solution and further stirred for 1 h at room temperature. The reaction mixture was filtered, washed with ethanol, and dried overnight under vacuum. Then, the material was dispersed in ethanol (10 mL), and a freshly prepared 0.05 M $NaBH_4$ ethanol solution (5 mL) was slowly added with vigorous stirring. After reduction for about 6 h, the mixture was filtered and washed thoroughly with deionized water and dried under vacuum at room temperature. The amount of Pd loaded in TiP was 0.12 mmol g^{-1} according to the ICP analysis.

In a typical reaction, *p*-iodoanisole (50 mg, 0.21 mmol) was reacted with a slight excess of boronic acid derivative (0.32 mmol) at 80 °C in DMF (2 mL) in the presence of K_2CO_3 (78 mg) and the catalyst (10 mg), and the reaction mixture was stirred under N_2. After reacting for about 2 h, the mixture was cooled to room temperature. The catalyst was filtered and washed with EtOAc. The pure product was isolated by column chromatography.

Characterizations

Powder X-ray diffraction (XRD) patterns were recorded on a Rigaku D/MAX 2500/PC X-ray diffractometer with Cu Kα radiation. N_2 adsorption–desorption isotherms at 77 K were measured on a Micromeritics Gemini V analyzer. Transmission electron microscopy (TEM) images were recorded with a JSM-3010 electron microscope. Scanning electron microscopy (SEM) images were recorded with a JSM-6700F electron microscope. Infrared (IR) measurements of the samples dispersed in KBr pellets were performed on a Perkin-Elmer spectrum 430 FTIR spectrometer. Solid-state ^{31}P MAS NMR experiments were taken on a Varian Infinity-plus 300 spectrometer operating at resonance frequency of 121.4 MHz, using a chemagnetic 4 mm double-resonance probe with a spinning rate of 8 kHz. ^{13}C MAS experiments were performed on a Varian Infinity-plus 400 spectrometer at a resonance frequency of 100.6 MHz using a 5 mm probe with a spinning rate of 8 kHz. The ^{13}C and ^{31}P chemical shifts were referenced to hexamethylbenzene (HMB) and 85% H_3PO_4, respectively.

Results and discussion

The compound PAC was prepared according to the synthetic route as shown in Scheme 1. Then, it was introduced into mesoporous titanium phosphonate through P–O–Ti covalent bonds by a one-pot condensation process by using CTAC as the surfactant (Scheme 2). After removing the surfactant, the material functionalized with carboxylic groups was obtained, marked as TiP. The content of PAC introduced in TiP determined by ICP analysis was 1.2 mol g^{-1} (Table 1).

Fig. 1 shows the X-ray diffraction patterns of TiP and TiP–Pd samples. It can be seen that the samples exhibit only one single broad low-angle reflection at $2\theta = 1.5°$ (Fig. 1a), indicating these hybrid materials have a "wormlike" mesoporous structure, which may be because the incorporation of PAC disturbed the formation of a well-ordered structure. With the incorporation of Pd nanoparticles, the intensity of the diffraction peak decreased and produces a large platform (Fig. 1b), suggesting more disordered structure of TiP–Pd.

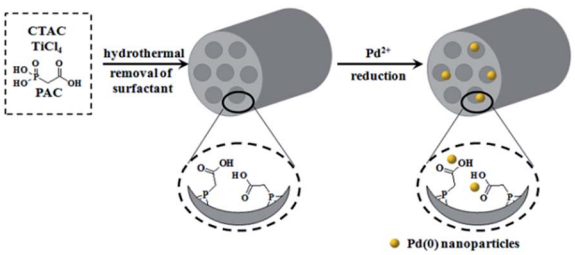

Scheme 2 The synthesized route of Pd nanoparticles supported on mesoporous titanium phosphonate.

Table 1 Physicochemical data for surfactant-extracted TiP and TiP–Pd

Sample	PAC mol g^{-1}	Pd mmol g^{-1}	S_{BET} m^2 g^{-1}	V cm^3 g^{-1}	D_{BJH} nm
TiP	1.2	—	458	0.53	2.6
TiP–Pd	1.2	0.12	300	0.33	2.5

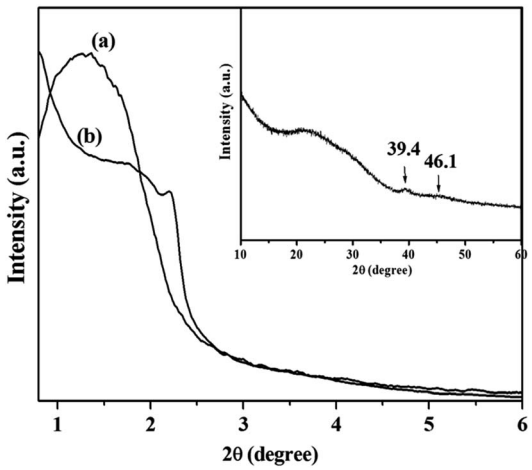

Fig. 1 Low angle XRD patterns of (a) TiP, and (b) TiP–Pd; (inset picture) wide angle of TiP–Pd.

The mesoporous structure was further confirmed by nitrogen adsorption at 77 K. Fig. 2 exhibits the N_2 adsorption–desorption isotherms and the corresponding pore size distribution curves of the materials. The isotherm of TiP is type IV according to the IUPAC classification, with the H_2 hysteresis loop at relative low pressure, characteristic of mesoporous materials. It has a specific BET surface area of 458 m^2 g^{-1}, pore volume of 0.53 cm^3 g^{-1} and corresponding pore size distribution displays only one well-defined peak centered at 2.6 nm. When Pd nanoparticles were incorporated into the material, its N_2 adsorption is lower and the pore size distribution is slightly decreased. The textural parameters of TiP and TiP–Pd are summarized in Table 1.

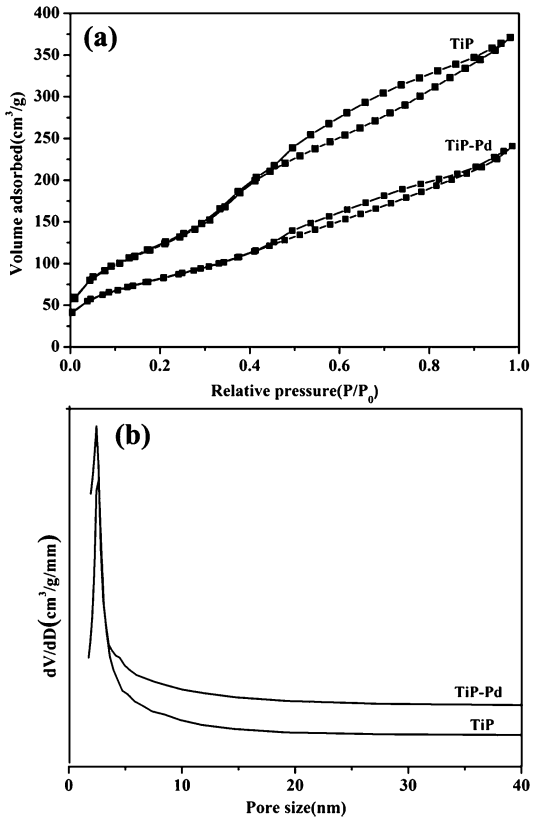

Fig. 2 (a) N_2 adsorption–desorption isotherms of TiP, TiP–Pd at 77 K and (b) corresponding pore size distribution curves (BJH method).

The spherical particles morphology of the material TiP was characterized by scanning electron microscopy (SEM) at different magnification, as shown in Fig. 3. The TEM micrograph (Fig. 4a) indicates that all the spherical particles are attached together and the presence of "wormlike" pore structure with about 2–3 nm, which is well consistent with XRD and N_2 adsorption. After loading Pd nanoparticles, there is no apparent change in the materials. As seen in the high magnification TEM image (Fig. 4b), the Pd nanoparticles are clearly distinguishable with the average size around 5 nm. This may be a consequence of the good stability effect of carboxylic groups to the palladium nanoparticles.

Fig. 5 is the FTIR spectra of TiP and PAC. According to the literature, the broad band at 3405 cm^{-1} can be attributed mainly to the –OH stretching vibration of the residual water. The strong band at 1718 cm^{-1} is attributed to the –COOH stretching vibration.[10] The wide band at 1034 cm^{-1} is the characteristic of Ti–O–P framework vibration. In brief, the FTIR data supports the conclusion that the organophosphonate PAC was successfully incorporated into the materials.

The maintenance of organic groups in the synthesized materials was further confirmed by ^{31}P and ^{13}C MAS NMR spectra (Fig. 6). Fig. 6a shows the ^{31}P MAS NMR spectra of TiP, presenting one peak at around 17 ppm, which can be assigned to the organic phosphorus species. In ^{13}C MAS NMR spectra, TiP shows a peak at 177 ppm attributed to the carbon in –COOH and $–COO^-$ groups. The signals at 36 ppm are related to the carbon atoms between the carboxyl group and the

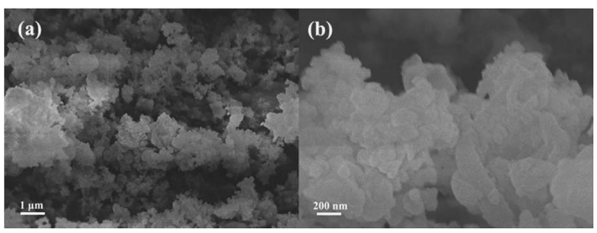

Fig. 3 The SEM images of the support TiP at different magnification.

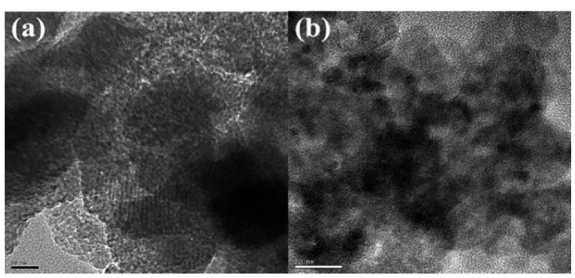

Fig. 4 The TEM images of (a) TiP, (b) TiP–Pd.

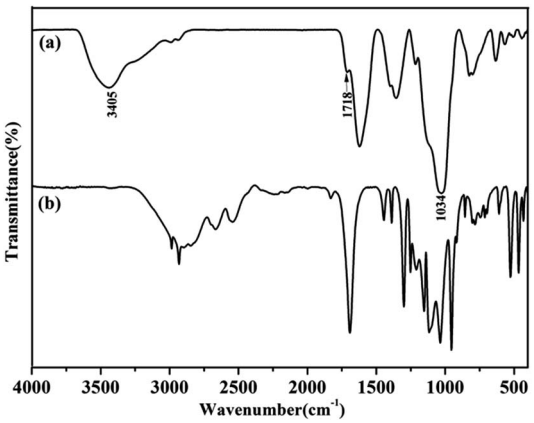

Fig. 5 The FTIR spectra of (a) TiP and (b) PAC sample.

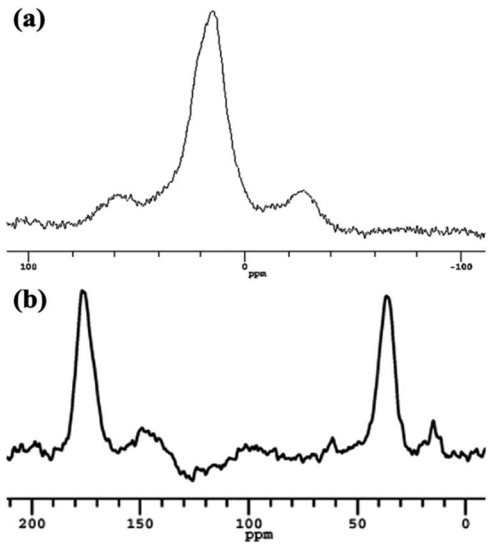

Fig. 6 ^{31}P MAS NMR spectra and ^{13}C MAS NMR spectra of TiP.

phosphonic group. In summary, the ^{31}P and ^{13}C MAS NMR data not only support the presence of organophosphonate in the structures, but also confirm the integrity of PAC after the template removal.

Carboxyl groups are uniformly distributed on the surface of TiP, which are good ligands for inorganic species. Thus, the synthesized materials may find potential applications in the fields of catalysis. In this work, we used this material to adsorb palladium(II) ion and reduce it to the zero valent examined by XRD (Fig. 1, inset) and X-ray photoelectron spectroscopic (XPS) technique (Fig. 7). We can see the appearance of diffraction peaks at 39.4°, 46.1° because of Pd in the metallic state (Fig. 1, inset). The presence of new Pd $3d_{3/2}$ and Pd $3d_{5/2}$ peaks at lower binding energies of 340.6 eV and 335.1 eV further indicates that Pd metals are formed.[11] Fig. 4b shows that the palladium nanoparticles are almost 5 nm, which may show catalytic activity on the Suzuki reaction. On the basis of the optimized reaction conditions, the coupling reactions between a range of *p*-iodoanisole and

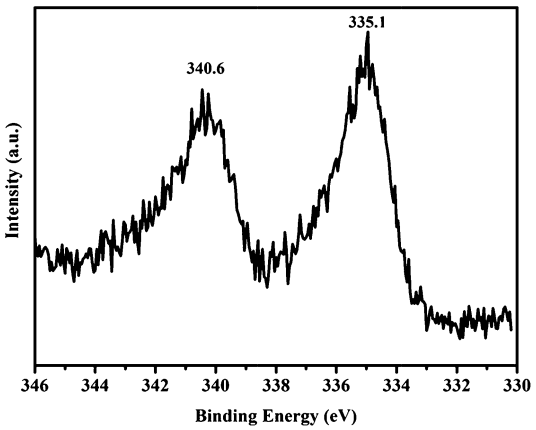

Fig. 7 XPS Pd 3d spectra of TiP–Pd samples.

Table 2 The coupling reactions of *p*-iodoanisole with various arylboronic acids

Entry	1	3	Yield (%)
1	H	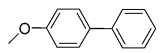	92
2	*p*-OMe	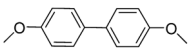	97
3	*o*-OMe	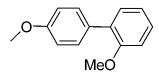	98
4	*p*-Ac	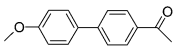	98
5	*p*-NO_2	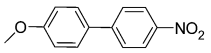	94

various arylboronic acids were carried out under an N_2 atmosphere. As shown in Table 2, the reaction afforded almost a 100% yield, showing that this material is an effective catalyst carrier for palladium nanoparticles. Furthermore, the catalyst can be reused for five cycles without significant loss in

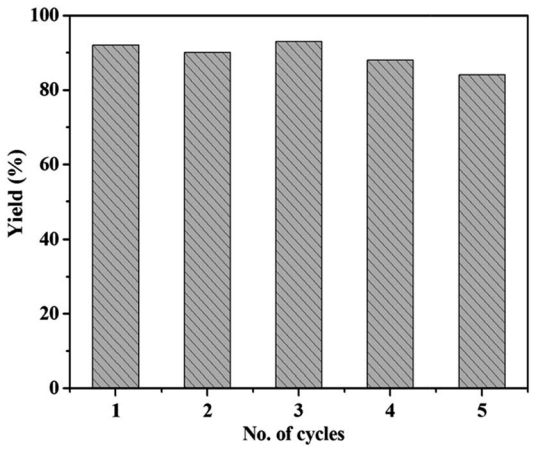

Fig. 8 The reusability of the catalyst.

activity by taking *p*-iodoanisole and phenylboronic acid, for example, demonstrating the efficiency of the catalyst (Fig. 8).

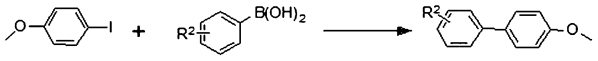

Conclusions

In conclusion, high surface area mesoporous titanium organophosphonate materials functionalized with a carboxyl group have been synthesized by the use of cationic surfactant CTAC as the structure-directing agent. Organic carboxyl groups maintain their integrity in the mesoporous materials, which was an effective ligand for palladium nanoparticles. The as-prepared nanosized palladium particles have a narrow size distribution (5 nm), showing high catalytic activity on the Suzuki reaction. Importantly, the catalyst can be reused for several times without the sharp loss of catalytic activity. Because the carboxyl group is a particularly useful reactive group, this material may find a wide range of potential applications in other fields, such as biomedicine *etc.*

Acknowledgements

This work is supported by the China Postdoctoral Science Foundation (801141002416).

Notes and references

1 A. P. Wight and M. E. Davis, *Chem. Rev.*, 2002, **102**, 3589; F. Hoffmann, M. Cornelius, J. Morell and M. Fröba, *Angew. Chem., Int. Ed.*, 2006, **45**, 3216; J. A. Melero, R. van Grieken and G. Morales, *Chem. Rev.*, 2006, **106**, 3790; A. Burns, H. Ow and U. Wiesner, *Chem. Soc. Rev.*, 2006, **35**, 1028.

2 R. K. Zeidan, S. J. Hwang and M. E. Davis, *Angew. Chem., Int. Ed.*, 2006, **45**, 6332; T. Kikukawa, K. Kuraoka, K. Kawabe, K. Yasuda, K. Hirao and T. Yazawa, *J. Am. Ceram. Soc.*, 2004, **87**, 504.

3 B. Lee, Y. Kim, H. Lee and J. Yi, *Microporous Mesoporous Mater.*, 2001, **50**, 77; X. B. Ma, J. Liu, L. S. Xiao, R. Chen, J. Q. Zhou and X. K. Fu, *J. Mater. Chem.*, 2009, **19**, 1098; B. Malvi, B. R. Sarkar, D. Pati, R. Mathew, T. G. Ajithkumar and S. S. Gupta, *J. Mater. Chem.*, 2009, **19**, 1409.

4 T. Y. Ma, X. Z. Lin and Z. Y. Yuan, *J. Mater. Chem.*, 2010, **20**, 7406; B. Z. Tian, X. Y. Liu, B. Tu, C. Z. Yu, J. Fan, L. M. Wang, S. H. Xie, G. D. Stucky and D. Y. Zhao, *Nat. Mater.*, 2003, **2**, 159; X. Shi, J. Liu, C. M. Li and Q. H. Yang, *Inorg. Chem.*, 2007, **46**, 7944.

5 T. Y. Ma, X. J. Zhang, G. S. Shao, J. L. Cao and Z. Y. Yuan, *J. Phys. Chem. C*, 2008, **112**, 3090; V. F. D. Álvaro and R. A. W. Johnstone, *J. Mol. Catal. A: Chem.*, 2008, **280**, 131.

6 S. Sumiya, Y. Kubota, Y. Oumi, M. Sadakane and T. Sano, *Appl. Catal., A*, 2010, **372**, 82; Z. Yan, S. Y. Tao, J. X. Yin and G. T. Li, *J. Mater. Chem.*, 2006, **16**, 2347.

7 S. Fiorilli, B. Camarota, D. Perrachon, M. C. Bruzzoniti, E. Garronez and B. Onidaz, *Chem. Commun.*, 2009, 4402; I. Kornarakis, G. Sopasis, C. J. Miliosb and G. S. Armatas, *RSC Adv.*, 2012, **2**, 9809; C. C. Ting, C. H. Chung and H. M. Kao, *Chem. Commun.*, 2011, **47**, 5897.

8 X. Shi, J. Yang and Q. H. Yang, *Eur. J. Inorg. Chem.*, 2006, 1936.

9 M. C. Bruzzoniti, A. Prelle, C. Sarzanini, B. Onida, S. Fiorilli and E. Garrone, *J. Sep. Sci.*, 2007, **30**, 2414; M. C. Bruzzoniti, C. Sarzanini, A. M. Torchia, M. Teodoro, F. Testa, A. Virga and B. Onida, *J. Mater. Chem.*, 2011, **21**, 369; H. Wang, Y. F. Yu, Q. W. Chen and K. Cheng, *Dalton Trans.*, 2011, **40**, 559.

10 S. C. Shen, P. S. Chow, S. G. Kim, K. W. Zhu and R. B. H. Tan, *J. Colloid Interface Sci.*, 2008, **321**, 365; S. Fiorilli, B. Onida, B. Bonelli and E. Garrone, *J. Phys. Chem. B*, 2005, **109**, 16725.

11 A. J. Amali and R. K. Rana, *Green Chem.*, 2009, **11**, 1781; F. W. Zhang, J. Jin, X. Zhong, S. W. Li, J. R. Niu, R. Li and J. T. Ma, *Green Chem.*, 2011, **13**, 1238.